Chapter 7

Effect of Heat Transfer on Swallowing of Food Bolus through Oesophagus with Dilating Peristaltic Wave: Application to cryosurgery

7.1 Introduction

Heat transfer refers to the exchange of thermal energy between physical systems. Transfer of thermal energy occurs from the body of higher temperature to the body of lower temperature. The rate of heat transfer depends on the temperature difference of nearby bodies and the physical properties of the medium through which heat transfer takes place. In the transport process of fluids, heat transfer takes place by the method of convection. In physiology, heat transfer analysis is applicable to get information about the properties of tissues. The flow of blood can be measured using a dilution technique, in which heat is either injected or generated locally and the thermal clearance is evaluated which gives flow rates. Recent development in application of hyperthermia, laser therapy and cryosurgery to destroy undesirable cancer tissues encourages the researchers to model the heat transfer effect in tissues.

Several decades back many authors (Pfeffer and Happel, 1964; Raju and Rathna, 1970; Victor and Shah, 1975; Zapryanov et al., 1980) presented heat transfer effect in tube flow but it was not peristaltic flow. Probably, first literature treating heat transfer in association with peristaltic flow was presented by Radhakrishnamacharya and Murty (1993).

They obtained closed form solutions for temperature, coefficient of heat transfer and velocity up to the second order by perturbation techniques. Vajravelu et al. (2007) discussed the interaction of peristalsis with heat transfer in a vertical porous annular region and formulated heat transfer at the wall and the pressure–flow relationship. Observations were that the heat transfer at the wall was affected significantly by the amplitude of the peristaltic wave but effect of pressure drop on flux was almost negligible for peristaltic waves of large amplitude. Mekheimer and Abdelmaboud (2008) investigated heat transfer and magnetic field on peristaltic transport of a Newtonian fluid in a vertical annulus with application to endoscope. Srinivas et al. (2009) studied the effects of wall slip conditions and heat transfer both on peristaltic flow of MHD Newtonian fluid in a porous channel with elastic wall properties under the assumptions of long wavelength and low-Reynolds number approximations. The influence of velocity-slip and thermal slip on peristaltic flow in an asymmetric channel was discussed by Hayat et al. (2010). Makinde and Chinyoka (2010) presented a model for transient heat transfer in channel flow and solved the governing nonlinear equations of momentum and energy transport numerically by finite difference method. Hayat et al. (2014) presented a study in order to show the effects of convective boundary conditions on peristaltic transport of a micropolar fluid in an asymmetric channel with heat source/sink. Prakash et al. (2018) discussed a numerical simulation to study the heat and flow characteristics of blood flow altered by electro-osmosis through the tapered micro-vessels assuming blood as non-Newtonian (micro-polar) nano-fluids. This study explored the nano-fluid dynamics in peristaltic transport as symbolized by heat transport in biological flows and also in gastro-intestinal motility enhancement. Misra et al. (2018) formulated a mathematical model to analyze the peristaltic transport of magneto hydrodynamic fluid associated with heat and mass transfer in an asymmetric channel. On the basis of this study, the authors reported that fluid velocity and the distributions of concentration and temperature are considerably influenced by Grashof number.

The mechanism of peristalsis, in oesophageal swallowing, has been the object of scientific research for long. The investigation of Li and Brasseur (1993) gave a boost to investigation on swallowing making the literature rich (Nguyen et al., 1997; Misra and Pandey, 2001; Nicosia and Brasseur, 2002; Toklu, 2011; Misra and Maiti, 2012; Pandey and Tiwari, 2017; Pandey and Singh, 2018a). Meanwhile, the report of high pressure zone in the

distal oesophagus by Kahrilas et al. (1995), followed by anatomical measurement of oesophageal wall thickness by Xia et al. (2009) in contracted and also in the dilated states, gave a new turn to research. Analysing the two reports, Pandey et al. (2017) concluded dilation of wave amplitude during propagation. But the interaction between heat transfer and peristalsis remained yet ignored in oesophageal swallowing.

Oesophageal diseases such as oesophageal cancer, oesophageal motility disorders and Barrett's oesophagus have brought the human health under threat in the modern society. The oesophageal heat transfer device, which is designed as a silicone orogastric tube with 3 lumens (Markota, 2016), is used for temperature management of adult survivors of cardiac arrest. Oesophageal cancer is one of the most lethal cancers and accounts for approximately 1% of all cancers (Kumbasar, 2002). Cryosurgery uses extreme cold liquid to destroy cancerous cells during surgery. Study of peristalsis in oesophagus with heat transfer effect may help cure those oesophageal diseases. Sreenadh et al. (2012) presented a model for the effect of heat transfer and wall properties of flexible walls in oesophageal swallowing. Tripathi (2012) and Tripathi et al. (2013) investigated mathematical model for swallowing of food bolus under the influence of heat transfer and derived the expressions for temperature field, axial velocity, volume flow rate, pressure gradient, local wall shear stress, stream function and reflux limit under the assumptions of long wavelength and low Reynolds number approximations. Authors assumed propagating train of boluses within the peristaltic wave with constant wave amplitude and considering the oesophagus as a channel. But, in view of Pandey et al. (2017), it looks more appropriate to examine the effect of heat transfer on swallowing of food bolus in an axisymmetric tube with dilating peristaltic wave amplitude. We prefer single bolus transport which is more frequent.

7.2 Mathematical Formulation

The equation of wall geometry of oesophageal tube, which is assumed as a circular cylindrical tube of finite length, due to propagation of a single peristaltic wave along it with dilating wave amplitude is modeled as

$$H'(x',t') = \begin{cases} a - \emptyset' e^{k'x'} cos^2 \frac{\pi}{\lambda}(x' - ct'), & \text{during } [t',\ t' + \frac{\lambda}{c}] \\ a - \emptyset' e^{k'x'}, & \text{otherwise} \end{cases} . \tag{7.1}$$

where $H', x', t', a, k', \emptyset', c$ and λ denote radial displacement of the wall from the centre line, axial coordinate, time parameter, radius of the tube, dilation parameter, amplitude of the wave, wave velocity and wavelength respectively (Fig. 7.1).

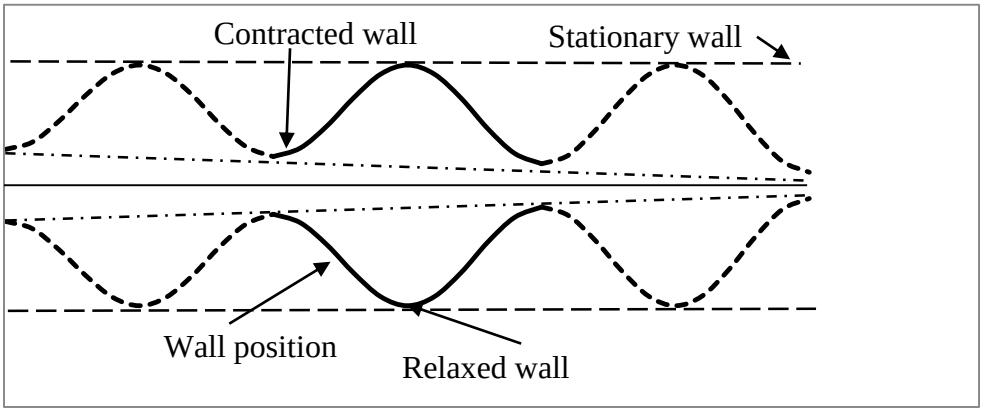

Fig. 7.1 *Schematic diagram of the flow under peristaltic waves of progressively dilating amplitude. Long dashed lines touching relaxed wall indicate stationary wall. The continuous solid wave indicates position of single bolus; similar boluses lagging behind or leading simply symbolize that the previous position and the future position of the bolus.*

The governing equations for unsteady axisymmetric flow of an incompressible Newtonian fluid with heat transfer and without body forces are given by

$$\rho\left(\frac{\partial}{\partial t'}+u'\frac{\partial}{\partial x'}+v'\frac{\partial}{\partial r'}\right)v' = -\frac{\partial p'}{\partial r'}+\mu'\left(\frac{1}{r'}\frac{\partial}{\partial r'}+\frac{\partial^2}{\partial r'^2}+\frac{\partial^2}{\partial x'^2}-\frac{1}{r'^2}\right)v', \tag{7.2}$$

$$\rho\left(\frac{\partial}{\partial t'}+u'\frac{\partial}{\partial x'}+v'\frac{\partial}{\partial r'}\right)u' = -\frac{\partial p'}{\partial x'}+\mu'\left(\frac{1}{r'}\frac{\partial}{\partial r'}+\frac{\partial^2}{\partial r'^2}+\frac{\partial^2}{\partial x'^2}\right)u'+\rho g\alpha(T'-T_0), \tag{7.3}$$

$$\rho c_p\left(\frac{\partial}{\partial t'}+u'\frac{\partial}{\partial x'}+v'\frac{\partial}{\partial r'}\right)T' = \kappa\left(\frac{1}{r'}\frac{\partial}{\partial r'}+\frac{\partial^2}{\partial r'^2}+\frac{\partial}{\partial x'^2}\right)T'+\Omega'. \tag{7.4}$$

The continuity equation is

$$\frac{\partial u'}{\partial x'}+\frac{1}{r'}\frac{\partial(r'v')}{\partial r'}=0\,. \tag{7.5}$$

where $\rho,\ u',\ p',\ v',\ r',\ g,\ \alpha,\ T',\ T_0,\ c_p,\ \kappa$ and Ω' are fluid density, axial velocity, pressure, radial velocity, radial coordinate, acceleration due to gravity, coefficient of linear

thermal expansion of the fluid, temperature at an arbitrary point of the fluid, temperature at the centre line, specific heat at constant pressure, thermal conductivity and constant heat addition or absorption respectively. The buoyancy force is approximated by the Boussinesq form (Bird et al., 1976) in the Eq. (7.3).

The various parameters are non-dimensionalised as follows:

$$\left.\begin{array}{c} x = \frac{x'}{\lambda}\ ,\ r = \frac{r'}{a}\ ,\ t = \frac{ct'}{\lambda}\ ,\ u = \frac{u'}{c}\ ,\ v = \frac{v'}{c\delta}\ ,\ \delta = \frac{a}{\lambda}\ , \\ H = \frac{H'}{a}\ ,\ k = k'\lambda,\ l = \frac{l'}{\lambda}\ ,\quad \phi = \frac{\emptyset'}{a}\ ,\quad p = \frac{p'\,a^2}{\mu' c\lambda}\ ,\ Q = \frac{Q'}{\pi a^2 c}, \\ R_e = \frac{\rho c\, a\delta}{\mu'},\ T = \frac{T'-T_0}{T_1-T_0}\ ,\ Gr = \frac{\rho g\alpha a^2(T_1-T_0)}{\mu' c},\ \Omega = \frac{a^2\Omega'}{\kappa(T_1-T_0)}\ . \end{array}\right\} \tag{7.6}$$

where $\delta, l'\ , Q', R_e\ ,\ T,\ T_1\ , Gr$ and Ω are wave number, length of the tube, volume flow rate, Reynolds number, dimensionless temperature, temperature at the wall, Grashof number and dimensionless heat parameter of the source or sink respectively.

Introducing the above mentioned non-dimensional parameters into Eqs. (7.1)-(7.5) and using the low Reynolds number and long wavelength approximations, wall equation (7.1) and governing Eqs. (7.2)-(7.5) reduce respectively to the following dimensionless forms

$$H(x,t) = \begin{cases} 1 - \emptyset e^{kx} cos^2\pi(x-t), & \text{during } [t,\ t+1\ ] \\ 1 - \emptyset e^{kx}, & \text{otherwise} \end{cases}. \tag{7.7}$$

$$\frac{\partial p}{\partial r} = 0, \tag{7.8}$$

$$\frac{\partial p}{\partial x} = \frac{1}{r}\frac{\partial}{\partial r}\left(r\frac{\partial u}{\partial r}\right) + \ GrT, \tag{7.9}$$

$$\frac{1}{r}\frac{\partial}{\partial r}(r\frac{\partial T}{\partial r}) + \Omega = 0, \tag{7.10}$$

$$\frac{\partial u}{\partial x} + \frac{1}{r}\frac{\partial (rv)}{\partial r} = 0. \tag{7.11}$$

The following dimensionless boundary conditions are imposed on the governing equations:

$$u(r,x,t)|_{r=H} = 0,\ \left.\frac{\partial u}{\partial r}\right|_{r=0} = 0,\ v(r,x,t)|_{r=0} = 0,\quad v(r,x,t)|_{r=H} = \frac{\partial H}{\partial t}\,, \tag{7.12}$$

$$\left.\frac{\partial T}{\partial r}\right|_{r=0} = 0, \quad T(r,x,t)|_{r=H} = 1. \tag{7.13}$$

7.3 Solution

Integrating Eq. (7.10) twice with respect to r, and using the first and second boundary conditions in (7.13) respectively, we get the temperature in the tube at any point as

$$T = 1 + \frac{\Omega}{4}(H^2 - r^2). \tag{7.14}$$

Integrating Eq. (7.9) too, with respect to r, by using Eq. (7.14), in view of Eq. (7.8) and second boundary condition in (7.12), we obtain the axial velocity gradient as

$$\frac{\partial u}{\partial r} = \frac{r}{2}\frac{\partial p}{\partial x} - Gr\left\{\frac{r}{2} + \frac{\Omega}{16}(2H^2 r - r^3)\right\},$$

which, on integrating once more with respect to r, and applying the first boundary condition in (7.12), gives the axial velocity as

$$u = \frac{1}{4}\frac{\partial p}{\partial x}(r^2 - H^2) + \frac{Gr}{64}\{16(H^2 - r^2) + \Omega(3H^4 - 4H^2 r^2 + r^4)\}. \tag{7.15}$$

Solving the continuity equation (7.11) by inserting the axial velocity given in Eq. (7.15) and applying the third boundary condition in (7.12), the radial velocity is given by

$$v = \frac{1}{16}\frac{\partial^2 p}{\partial x^2}(2H^2 r - r^3) - \frac{rH}{4}\frac{\partial p}{\partial x}\frac{\partial H}{\partial x} - \frac{GrH}{32}\frac{\partial H}{\partial x}\{8r + \Omega(3H^2 r - r^3)\}. \tag{7.16}$$

In view of the forth boundary condition in (7.12), Eq. (7.16) gives

$$\frac{\partial^2 p}{\partial x^2} - \frac{4}{H}\frac{\partial H}{\partial x}\frac{\partial p}{\partial x} = \frac{16}{H^3}\frac{\partial H}{\partial t} + \frac{4Gr}{H}\frac{\partial H}{\partial x}\left(1 + \frac{\Omega H^2(s,t)}{4}\right),$$

which, on integrating with respect to x, yields

$$\frac{\partial p}{\partial x} = \frac{g(t) + 16\int_0^x H\frac{\partial H}{\partial t}dx + Gr\left\{H^4(x,t) - H^4(0,t) + \frac{\Omega}{6}\left(H^6(x,t) - H^6(0,t)\right)\right\}}{H^4}, \tag{7.17}$$

where $g(t)$ is an arbitrary function of t.

Integrating Eq. (7.17) from the inlet to an arbitrary point along the axis of the oesophagus, we obtain the axial pressure as

$$p(x,t) = p(0,t) + \int_0^x \left\{ \frac{g(t)+16\int_0^{s_1} H(s,t)\frac{\partial H(s,t)}{\partial t}ds + Gr\left\{H^4(s_1,t)-H^4(0,t)+\frac{\Omega}{6}\left(H^6(s_1,t)-H^6(0,t)\right)\right\}}{H^4(s_1,t)} \right\} ds_1. \quad (7.18)$$

Now $g(t)$ is evaluated by putting $x = l$ in Eq. (7.18), which is given by

$$g(t) = \frac{p(l,t)-p(0,t)-\int_0^l \left\{16\int_0^{s_1} H(s,t)\frac{\partial H(s,t)}{\partial t}ds + Gr\left\{H^4(s_1,t)-H^4(0,t)+\frac{\Omega}{6}\left(H^6(s_1,t)-H^6(0,t)\right)\right\}\right\} H^{-4}(s_1,t)ds_1}{\int_0^l \frac{1}{H^4}dx}. \quad (7.19)$$

7.3.1 Pressure rise vs. time-averaged volume flow rate

The volume flow rate for single wave transport is defined as

$Q(x,t) = 2\eta \int_0^H urdr$, where $\eta = \frac{l}{\lambda}$. In view of Eq. (7.15) it yields on integration,

$$Q(x,t) = \eta \frac{H^4}{8}\left\{\frac{Gr}{6}(6+\Omega H^2) - \frac{\partial p}{\partial x}\right\} . \quad (7.20)$$

Following are the existing relations between the wave and laboratory frames:

$$\left.\begin{aligned} &X = x - t,\ R = r,\ U(R,X) = u(r,x,t) - 1, \\ &V(R,X) = v(r,x,t), \qquad q = Q(x,t) - H^2. \end{aligned}\right\} \quad (7.21)$$

Note that the parameters on the left side are in the wave frame and those on the right side are in the laboratory frame.

The time-averaged volume flow rate over a period in the laboratory frame for single wave propagation is defined to be

$$\bar{Q}(x) = \frac{1}{\eta}\int_0^{\eta} Q dt ,$$

which, in view of fifth relation of Eq. (7.21), yields

$$Q = \bar{Q} + H^2 - \frac{1}{\eta}\int_0^{\eta} H^2 dt , \quad (7.22)$$

Hence, from Eq. (7.20) we have

$$\frac{\partial p}{\partial x} = \frac{Gr}{6}(6 + \Omega H^2) - \frac{8}{\eta H^4}\left(\bar{Q} + H^2 - \frac{1}{\eta}\int_0^{\eta} H^2 dt\right). \tag{7.23}$$

The pressure at an arbitrary point along the length of the oesophagus, in terms of the time averaged volume flow rate, is determined by integrating Eq. (7.23) from the inlet to an arbitrary point on the axis, as

$$p(x,t) = p(0,t) + \int_0^x \left\{\frac{Gr}{6}(6 + \Omega H^2) - \frac{8}{\eta H^4}\left(\bar{Q} + H^2 - \frac{1}{\eta}\int_0^{\eta} H^2 dt\right)\right\} dx. \tag{7.24}$$

In terms of the time averaged volume flow rate, pressure rises per wavelength at the rate

$$\Delta P1 = p(1,t) - p(0,t) = \int_0^1 \left\{\frac{Gr}{6}(6 + \Omega H^2) - \frac{8}{\eta H^4}\left(\bar{Q} + H^2 - \frac{1}{\eta}\int_0^{\eta} H^2 dt\right)\right\} dx. \tag{7.25}$$

7.3.2 Local wall shear stress vs. time-averaged volume flow rate

The local wall shear stress at the wall is defined as

$$\tau_w(x,t) = \frac{\partial u}{\partial r}\Big|_{r=H},$$

which, in view of Eq. (7.15), gives

$$\tau_w(x,t) = \frac{H}{2}\frac{\partial p}{\partial x} - \frac{GrH}{16}(8 + \Omega H^2), \tag{7.26}$$

Using Eq. (7.23), it yields the local wall shear stress, in terms of the time-averaged volume flow rate, as

$$\tau_w(x,t) = \frac{Gr\Omega H^3}{48} - \frac{4}{\eta H^3}\left(\bar{Q} + H^2 - \frac{1}{\eta}\int_0^{\eta} H^2 dt\right). \tag{7.27}$$

7.4 Results and Discussions

In order to discuss qualitative effects of the various parameters involved in the present analysis we assume single bolus swallowing in the oesophagus capable of accommodating four boluses in its length at a time. Single bolus transport is a more practical phenomenon. A bolus is assumed to be contained within one peristaltic wavelength but may appear at different spatial positions at different instants. We randomly choose four time instants $t =$

$0.26, 0.93, 1.69$ and 2.78. The numerical evaluations of the analytical results are obtained for pressure, pressure rise per wavelength and local wall shear stress by setting zero pressure at the two ends of the oesophagus. We have plotted Figs. 2 – 5 to examine the effects of the Grashof number and the heat source/sink parameter on pressure, pressure rise per wavelength and local wall shear stress.

Figures 2(a)-(d) nicely describe the changes that take place in the pressure distribution in the oesophagus undergoing peristalsis with the variation in the Grashof number, Gr $(= 0.0, 3.5, 7.0)$ with $l = 4, \phi = 0.7, k = 0.01$ and $\Omega = 3.0$ at various instants (a) $t = 0.26$, (b) $t = 0.93$, (c) $t = 1.69$ and (d) $t = 2.78$. At t = 0.26, it is observed that the greater the Grashof number, the lower is the drop in pressure revealing a smaller requirement of pressure (Fig. 2a). On increasing the effect of heat transfer, it reveals that pressure reduces. Fig. 2(b) depicts the pressure distribution for position of bolus at $t = 0.93$. One may note that pressure increases steadily behind the bolus which restrains the bolus from any possible retrograde motion. Pressure reaches a peak and then falls sharp to a minimum which again rises progressively to attain the final zero pressure. Thus, only one pair of peak and trough of pressure is seen throughout the length of oesophagus at a time. Similar is the observation when the positions of the bolus are at $t = 1.69$ and $t = 2.78$ with some differences of magnitude observed over time instants. Another remarkable observation is that the difference between the maximum and minimum pressures at end close to the cardiac sphincter is higher than that at the proximal end, which is expected due to dilating wave amplitude. Pressure distribution in this single bolus case is quite different from that for the train wave case as reported by Tripathi (2012) and Tripathi et al. (2013).

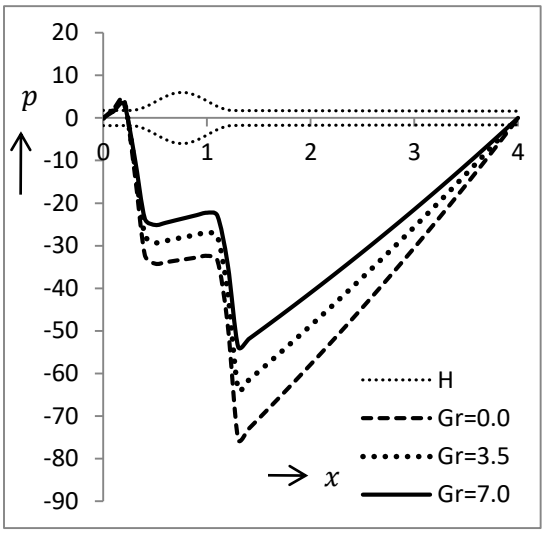

(a) $t = 0.26$

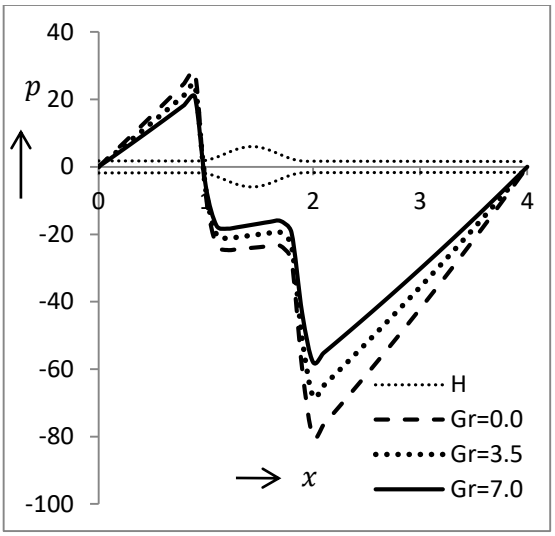

(b) $t = 0.93$

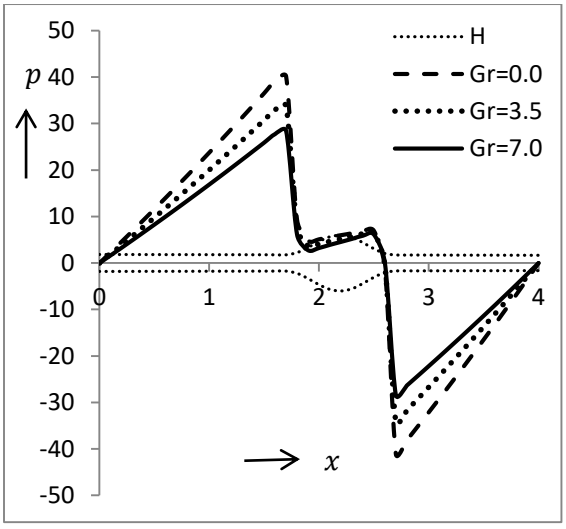

(c) $t = 1.69$

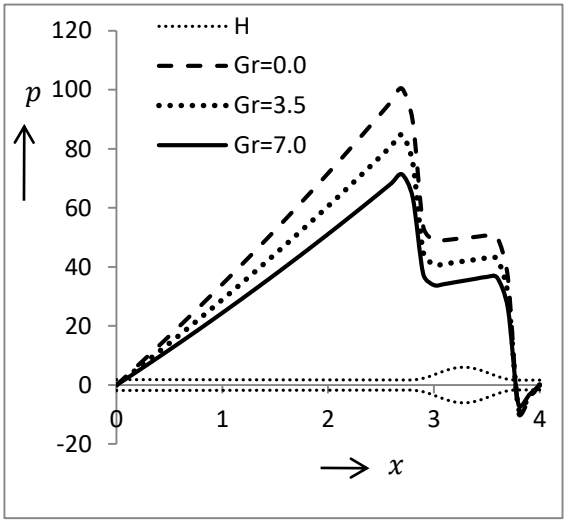

(d) $t = 2.78$

Fig. 7.2(a-d) *Pressure variation versus axial distance for* $Gr = 0.0, 3.5, 7.0, l = 4, \phi = 0.7, k = 0.01, \Omega = 3.0$ *and at various instants* (a) $t = 0.26$, (b) $t = 0.93$, (c) $t = 1.69$, (d) $t = 2.78$.

Figures 7.3(a)-(d) give an idea of the change in pressure distribution along the axis for $\Omega = 0.0, 4.0, 8.0$ with $l = 4, \phi = 0.7, k = 0.01, Gr = 2.0$ and at various instants of time $t = 0.26,\ 0.93,\ 1.69$ and 2.78. It is observed that an increment in Ω reduces the pressure irrespective of time.

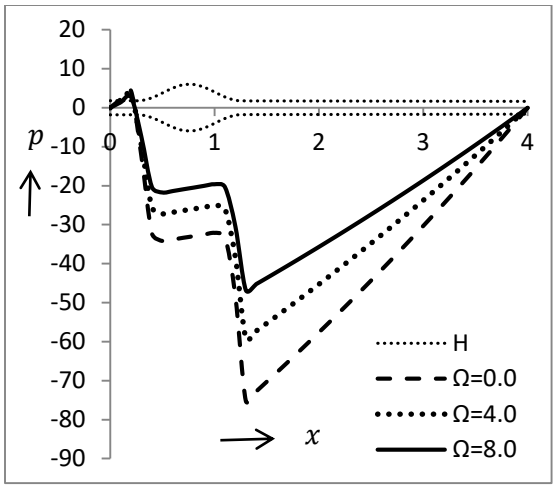

(a) $t = 0.26$

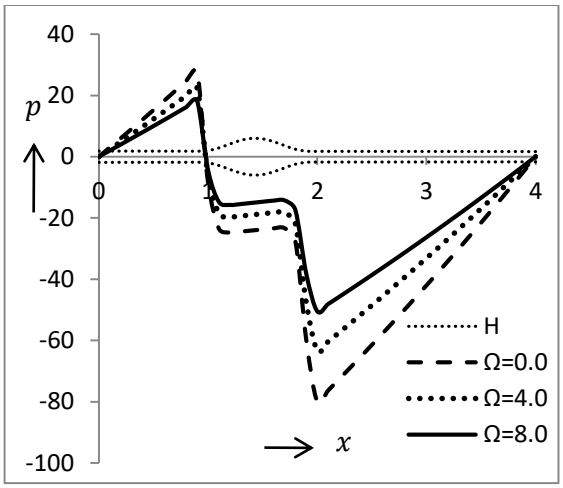

(b) $t = 0.93$

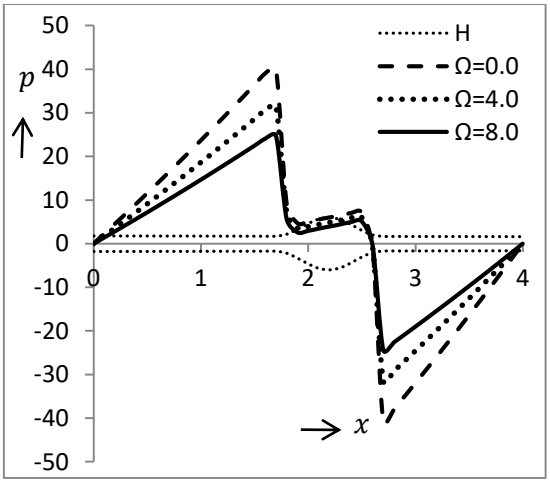

(c) $t = 1.69$

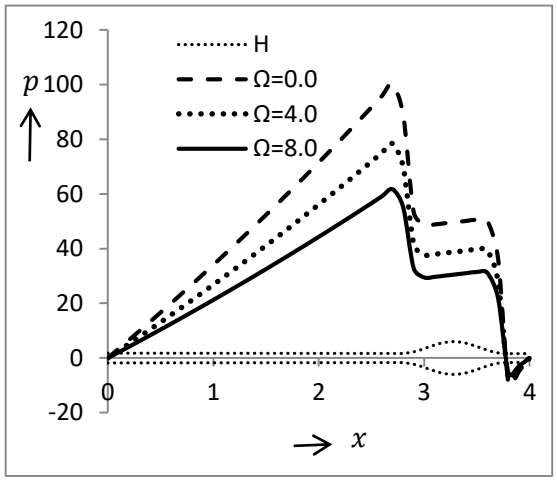

(d) $t = 2.78$

Fig. 7.3(a-d) *Pressure variation versus axial distance for* $\Omega = 0.0, 4.0, 8.0, l = 4, \phi = 0.7, k = 0.01, Gr = 2.0$ *and at various instants* (a) $t = 0.26$, (b) $t = 0.93$, (c) $t = 1.69$, (d) $t = 2.78$.

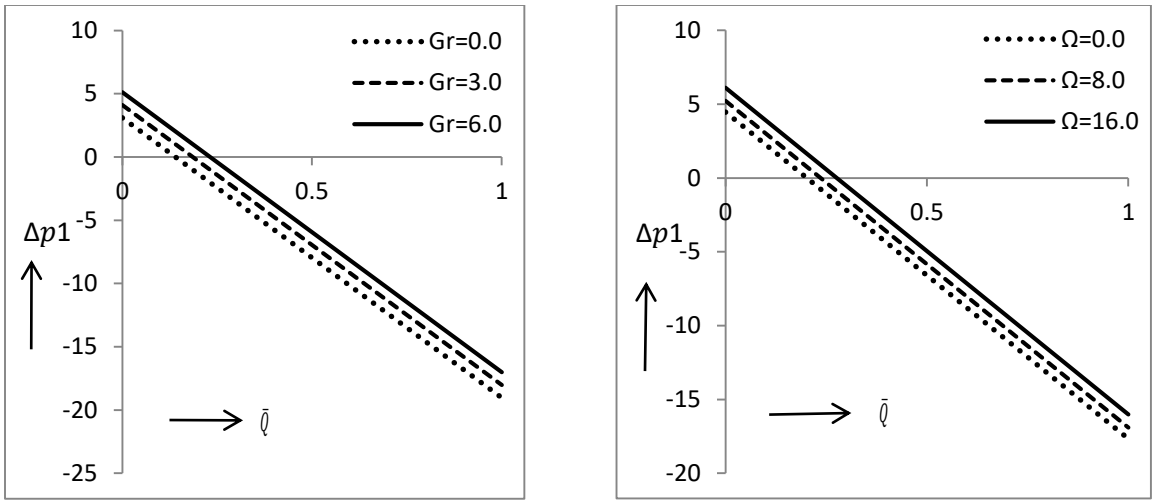

(a) (b)

Fig. 7.4(a-b) *Pressure rise per wavelength versus time averaged volume flow rate for* $l = 4$, $\phi = 0.6,\ k = 0.01,\ t = 1.5$ (a) $Gr = 0.0, 3.0, 6.0$ and $\Omega = 4.0$ (b) $\Omega = 0.0, 8.0, 16.0$ and $Gr = 5.0$.

Figures 7.4(a)-(b) present the graphs of pressure rise per wavelength versus flow rate, which describe the effects of Grashof number and heat source/sink parameter. We set $Gr = 0.0, 3.0, 6.0$ and $\Omega = 4.0$ for Fig. 7.4(a) and $\Omega = 0.0, 8.0, 16.0$ and $Gr = 5.0$ for Fig. 7.4(b). Other parameters are set as $l = 4,\ \phi = 0.6,\ k = 0.01$ and $t = 1.5$ for both the figures. Examining the behaviour of the depicting figures, we see that the magnitude of the pressure rise per wavelength increases with either of the Grashof number and the heat source/sink parameter before attaining a particular value of the time-averaged volume flow rate but the trend reverses beyond that. It is also observed that pressure rise per wavelength varies linearly with the time-averaged volume flow rate.

The characteristics of the local wall shear stress varying with the time-averaged volume flow rate, at the fixed axial coordinate $x = 0.93$ for $Gr = 0.0,\ 5.0,\ 10.0$ and $\Omega = 0.0,\ 5.0,\ 10.0$, is depicted in Fig. 7.5 and Table 7.1. It is observed that the local wall shear stress varies inversely with the time-averaged volume flow rate. The effects of variation in Gr and Ω on the local wall shear stress is not significant, hence not visible in Figs. 7.5(a)-(b). Therefore, it is given in Table 7.1. Analysing Fig. 7.5, we infer that τ_w is positive or negative depending on $\bar{Q}$.

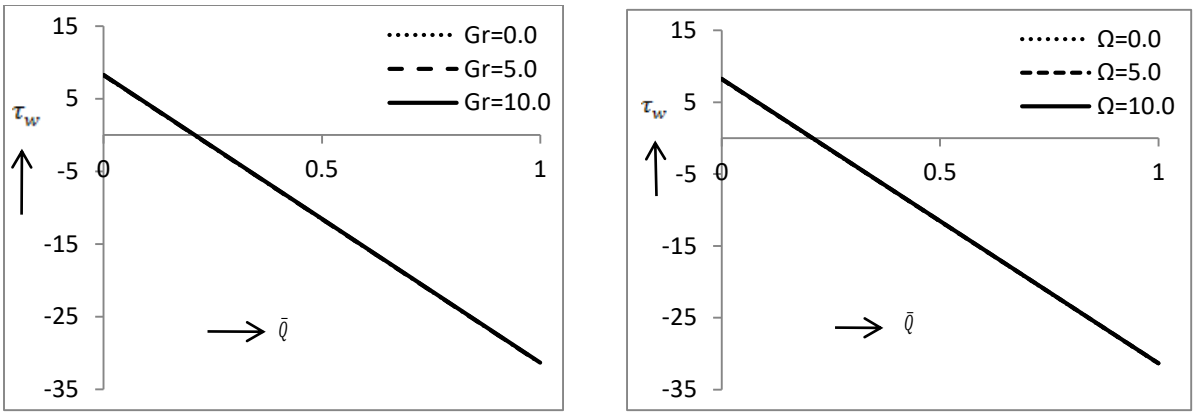

(a) (b)

Fig. 7.5(a-b) *Local wall shear stress versus time averaged volume flow rate for* $l = 4,\ \phi = 0.7,\ k = 0.01,\ x = 0.93, t = 0.93$ (a) $Gr = 0.0, 5.0, 10.0$ and $\Omega = 5.0$ (b) $\Omega = 0.0, 5.0, 10.0$ and $Gr = 5.0$.

$\bar{Q}$	0.0	0.2	0.4	0.6	0.8	1.0
τ_w at $Gr = 0.0, \Omega = 5.0$	8.2042	0.2904	-7.6233	-15.5371	-23.4509	-31.3647
τ_w at $Gr = 5.0, \Omega = 5.0$	8.2253	0.3115	-7.6022	-15.5161	-23.4298	-31.3436
τ_w at $Gr = 10.0, \Omega = 5.0$	8.2463	0.3325	-7.5812	-15.4950	-23.4088	-31.3226
τ_w at $Gr = 5.0, \Omega = 0.0$	8.2042	0.2904	-7.6233	-15.5371	-23.4509	-31.3647
τ_w at $Gr = 5.0, \Omega = 5.0$	8.2253	0.3115	-7.6022	-15.5161	-23.4298	-31.3436
τ_w at $Gr = 5.0, \Omega = 10.0$	8.2463	0.3325	-7.5812	-15.4950	-23.4088	-31.3226

Table 7.1 *Local wall shear stress versus time averaged volume flow rate for* $l = 4,\ \phi = 0.7,\ k = 0.01,\ x = 0.93$ *and* $t = 0.93$.

7.5 Conclusions

A mathematical model for the study of heat transfer in swallowing of food bolus through the oesophagus is presented analytically. The numerical evaluation of analytical results is done for plotting graphs. It is observed that pressure drops when either of the Grashof number and the heat source/sink parameter increases along the oesophageal axis. We infer from that

smaller is the requirement of pressure to swallow when heat propagates in the oesophagus. Pressure-rise- per-wavelength increases with either of the Grashof number and the heat source/sink parameter before attaining a particular value of the time-averaged volume flow rate but the trend reverses beyond that. The Grashof number and the heat source/sink parameter have an insignificant impact on local wall shear stress. Pressure rise per wavelength and local wall shear stress vary inversely with the time-averaged volume flow rate. It is worthwhile to mention that the study of heat transfer effect on oesophageal swallowing is quite promising for oesophageal cancer treatment.